Sensors and Materials, Vol. 37, No. 2 (2025) 539–546
MYU Tokyo

S & M 3930

Development of Eu-doped $Gd_3Al_3Ga_2O_{12}$ Nanoparticles for *in vivo* Applications

Masanori Koshimizu,[1,2*] Kazuki Tanahashi,[2] Yutaka Fujimoto,[3] and Keisuke Asai[3]

[1]Research Institute of Electronics, Shizuoka University, 3-5-1 Johoku, Chuo-ku, Hamamatsu 432-8011, Japan
[2]Electronics and Materials Science Department, Faculty of Engineering, Shizuoka University, 3-5-1 Johoku, Chuo-ku, Hamamatsu 432-8011, Japan
[3]Department of Applied Chemistry, Graduate School of Engineering, Tohoku University, 6-6-07 Aoba, Aramaki, Aoba-ku, Sendai 980-8579, Japan

(Received November 5, 2024; accepted December 16, 2024)

Keywords: scintillator, nanoparticle, garnet, *in vivo*

Red-emitting scintillator nanoparticles based on Eu-doped $Gd_3Al_3Ga_2O_{12}$ were developed. Nanoparticles of 100–300 nm size were successfully obtained. The photoluminescence (PL) and X-ray-induced radioluminescence spectra had sharp peaks in the wavelength region of 590–820 nm, which are attributed to the 4f–4f transitions of Eu^{3+} ions. The Eu concentration dependence of the emission properties was investigated. The PL quantum yield was the highest (98.4%) for the Eu concentration of 5% with respect to (Gd + Eu). Judged from the high PL quantum yield and radioluminescence in the red wavelength region, the development of the red-emitting nanoparticle scintillators was successful.

1. Introduction

Scintillators are luminescent materials that can be used for real-time radiation detection. They are combined with photon detectors such as photomultiplier tubes or photodiodes to form scintillation detectors. Scintillators are categorized as organic[(1–3)] or inorganic[(4,5)] with some exceptions being organic–inorganic hybrid compounds having a low-dimensional structure[(6–9)] or organic–inorganic composites.[(10–13)] Organic scintillators have relatively low scintillation light yields and fast decay, whereas inorganic scintillators have high scintillation light yields and slow decay in general. Among inorganic scintillators, there are oxide-[(14–30)] and halide-based[(31–39)] single crystalline scintillators. Oxide-based single crystalline scintillators have lower scintillation light yields than halide-based ones, whereas the chemical stability of oxide scintillators is superior to that of halide scintillators.

In addition to the applications of radiation detection, the use of scintillators in biological bodies or cells, i.e., *in vivo* applications, has been expanding recently.[(40,41)] For example, it has been reported that the behavior of a mouse was successfully controlled by X-ray irradiation from outside the body of the mouse.[(42)] In this study, scintillator microparticles were coupled with photoreceptor molecules and neurons, and the scintillation from the microparticles induced by

*Corresponding author: e-mail: koshimizu.masanori@shizuoka.ac.jp
https://doi.org/10.18494/SAM5448

ISSN 0914-4935
https://myukk.org/

X-rays was used as the light source within the living body. For this application, we have developed Ce-doped $Gd_3Al_3Ga_2O_{12}$ (GAGG) nanoparticle scintillators.[43] The developed nanoparticles were successfully applied for remotely activating light-sensitive proteins in biological tissue.[44]

In this study, we aim to develop nanoparticle scintillators exhibiting scintillation in the red wavelength region to be used for photoreceptor molecules having absorption wavelength in the red region. Similarly to a previous study,[43] GAGG was chosen as the host compound because of its high density and effective atomic number, which results in efficient X-ray stopping. Eu^{3+} ions were chosen as luminescent centers to realize red emission via the 4f–4f transitions of Eu^{3+} ions.

2. Materials and Methods

L(+)-tartaric acid (99.5%, Fujifilm Wako Pure Chemical), $Gd(NO_3)_3{\cdot}6H_2O$ (99.99%, Sigma-Aldrich), $Al(NO_3)_3{\cdot}9H_2O$ (99.9%, Fujifilm Wako Pure Chemical), $Ga(NO_3)_3{\cdot}nH_2O$ (99.999%, Kojundo Chemical Laboratory), and $Eu(NO_3)_3{\cdot}6H_2O$ (99.9%, Sigma Aldrich) were used as raw materials without further purification. The number of hydrated water molecules, n, of $Ga(NO_3)_3{\cdot}nH_2O$ was estimated by inductively coupled plasma optical emission spectroscopy (ICP-OES) analysis.

Eu-doped GAGG nanoparticles were synthesized according to procedures described in previous papers.[43,45] Tartaric acid was dissolved in distilled water at 0.6 M. Subsequently, metal nitrates were dissolved in the solution at the stoichiometric ratio [(Gd + Eu):Al:Ga=3:3:2] with the total metal concentration of 0.3 M. The solution was stirred for 24 h at room temperature and for 2 h at 80 °C in a beaker covered with Al foil. Subsequently, the Al foil was removed, and the beaker was placed in an oil bath at 80 °C to obtain a dry gel. Finally, the dry gel was calcined at 1300 °C for 6 h to obtain nanoparticles.

The X-ray diffraction (XRD) patterns of the nanoparticles were obtained using a diffractometer (RINT-2000, Rigaku) equipped with a Cu target operated at 40 kV and 20 mA to investigate the lattice structure of the nanoparticles. The morphology of the nanoparticles was investigated by transmission electron microscopy (TEM; JEM-2100F, JEOL). Photoluminescence (PL) excitation–emission contour maps were obtained and absolute PL quantum yields (QYs) were estimated using a PL QY measurement instrument (C11347, Hamamatsu). X-ray-induced radioluminescence (XRL) spectra were obtained using an X-ray generator (SA-HFM3, Rigaku) operated at 40 kV and 40 mA as the excitation source. The scintillation photons from the samples were delivered to a CCD detector equipped with a monochromator (QE-Pro, Ocean Optics) via an optical fiber.

3. Results and Discussion

The XRD patterns of the Eu-doped GAGG nanoparticles with different Eu concentrations are shown in Fig. 1. The reference diffraction patterns of $Gd_3Al_2Ga_3O_{12}$,[46] β-Ga_2O_3,[47] and $GdAlO_3$[48] are also presented. Note that Eu 100 mol% corresponds to $Eu_3Al_3Ga_2O_{12}$ composition. All the diffraction patterns are consistent with that of the $Gd_3Al_2Ga_3O_{12}$ reference

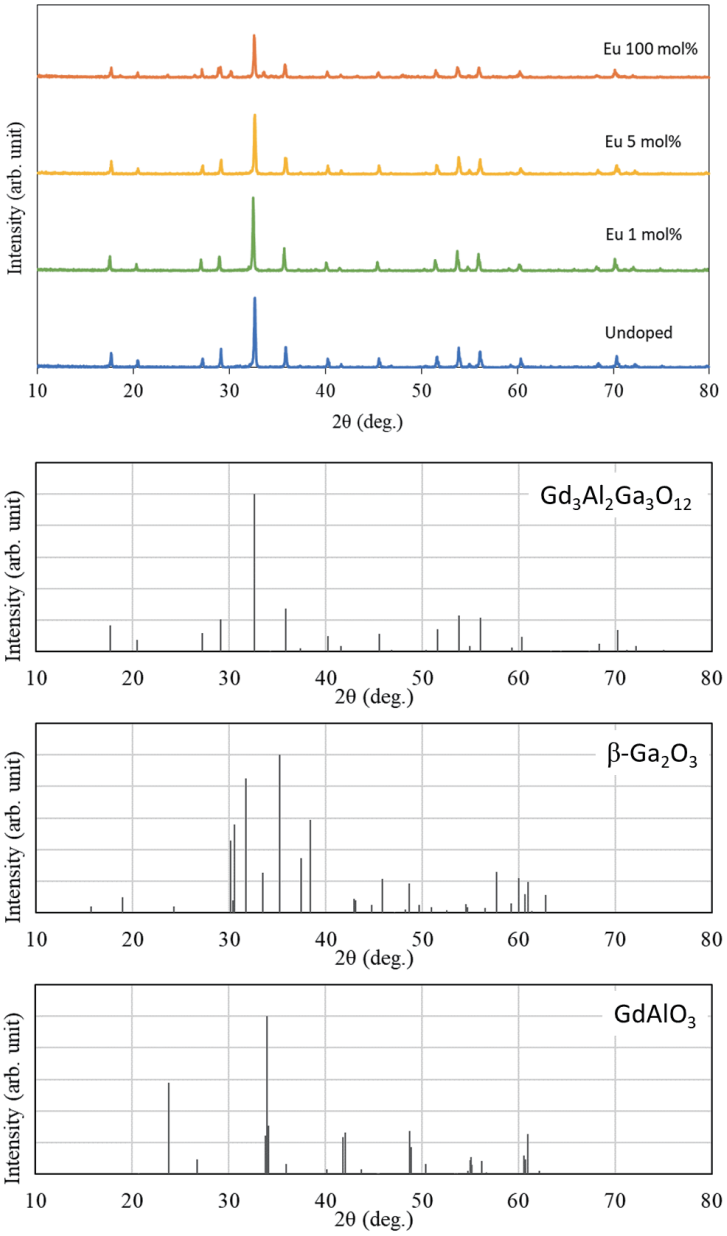

Fig. 1. (Color online) XRD patterns of nanoparticles with (Gd + Eu):Al:Ga=3:3:2 with different Eu concentrations with respect to (Gd + Eu) and reference patterns of $Gd_3A_{l2}Ga_3O_{12}$,[46] β-Ga_2O_3,[47] and $GdAlO_3$.[48]

except for the Eu 100 mol% sample, whose diffraction pattern is mostly consistent with that of the $Gd_3Al_2Ga_3O_{12}$ reference with small diffraction peaks at 30.14 and 33.60°, which may be attributed to the β-Ga_2O_3 phase. This result indicates that the nanoparticles of different Eu concentrations were in GAGG single phase except for the Eu 100 mol% sample, which is mostly composed of the GAGG phase. The secondary β-Ga_2O_3 phase observed for the Eu 100 mol% sample is not attributable to the stoichiometry of the metal species in the raw materials. In our previous work on Ce-doped GAGG, β-Ga_2O_3 was also found as a minor phase, and the intensity

of the diffraction peak at 30.4°, which is attributed to the β-Ga_2O_3 phase, increased with the duration of stirring at room temperature.[31] The minor β-Ga_2O_3 phase observed for the Eu 100 mol% sample may be attributable to the Ga-rich domain formed during stirring at room temperature, which results in the β-Ga_2O_3 phase. No other crystalline phases, such as the $GdAlO_3$ perovskite phase, which is sometimes observed in rare-earth garnet, were observed in the XRD patterns. This result is consistent with that in a previous paper on Eu-doped GAGG single crystals grown by a floating zone melting method:[49] single-phase crystals were successfully obtained for Eu concentrations up to 15 mol%. This result is also reasonable from the viewpoint of similar ionic radii of Gd^{3+} (0.1053 nm) and Eu^{3+} (0.1066 nm) ions in their 8-coordinate site.[50]

The TEM image of an Eu-doped GAGG nanoparticle with a Eu concentration of 5 mol% is shown in Fig. 2. The TEM image of the nanoparticle shown in Fig. 2 is a typical one. The size is 50–300 nm. The nanoparticles typically have a spheroid shape. The shape and size of the nanoparticles are similar to those of Ce-doped GAGG nanoparticles.[43]

The PL excitation–emission maps of undoped and Eu-doped GAGG nanoparticles with a Eu concentration of 5 mol% are shown in Fig. 3. The excitation–emission maps of the nanoparticles with other Eu concentrations are similar. A weak emission band at ~800 nm is observed in both samples with excitation at ~270 nm. The peak and excitation wavelengths are similar to those of previous papers on Fe-doped[51] and nominally undoped[52] $Y_3Al_5O_{12}$ (YAG). On the basis of this similarity, the emission band at around 790 nm is attributed to Fe impurity. The explanation in the paragraph of the PL excitation–emission map is revised. In the Eu-doped sample, we observed excitation peaks at around 260, 320, 390, 460, and 530 nm. Among them, the broad excitation peak at around 260 nm can be attributed to charge-transfer excitation from O^{2-} to Eu^{3+}, similarly to the case of Eu^{3+}-doped YAG powder.[53] The excitation peak at 320 nm can be attributed to the $^7F_0 \rightarrow {}^5L_8$ transition of Eu^{3+} ions, similarly to the case of Eu^{3+}-doped YAG nanoparticles.[54] The excitation peaks at around 390, 460, and 530 nm are attributed to the

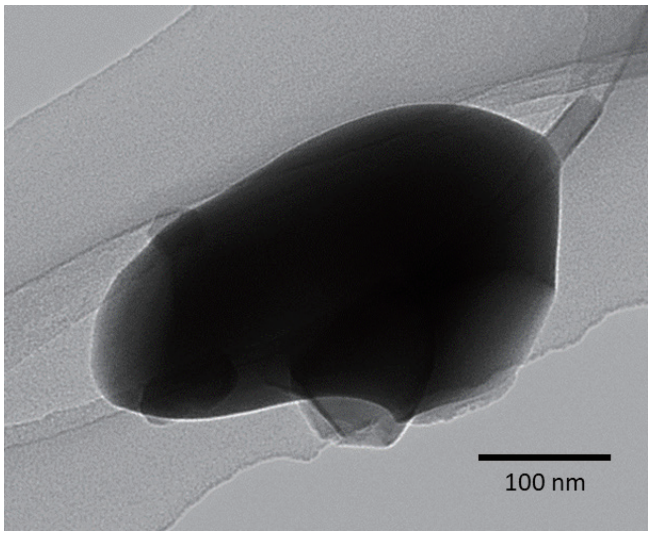

Fig. 2. TEM image of Eu-doped GAGG nanoparticle with Eu concentration of 5 mol%.

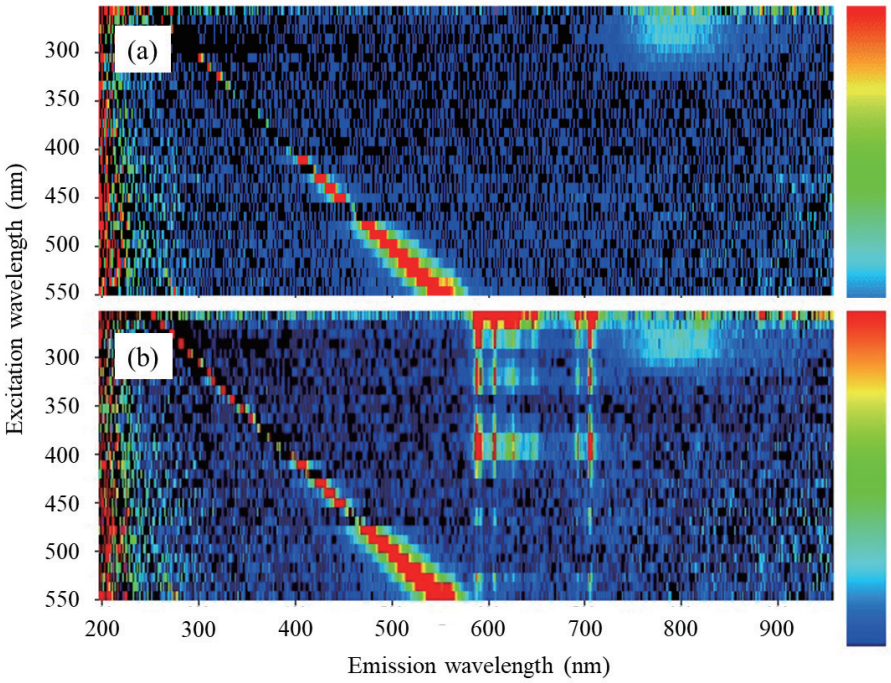

Fig. 3. (Color online) Excitation-emission maps of (a) undoped and (b) Eu-doped GAGG nanoparticles with Eu concentration of 5 mol%.

$^7F_0 \rightarrow {}^5L_6$, $^7F_0 \rightarrow {}^5D_2$, and $^7F_0 \rightarrow {}^5D_1$ electronic transitions of Eu^{3+}, respectively.[55] Sharp emission bands of the Eu-doped sample were observed at around 590, 610, 630, 650, 690, and 710 nm. They are attributed to $^5D_0 \rightarrow {}^7F_1$, $^5D_0 \rightarrow {}^7F_2$, $^5D_0 \rightarrow {}^7F_2$, $^5D_0 \rightarrow {}^7F_3$, $^5D_0 \rightarrow {}^7F_4$, and $^5D_0 \rightarrow {}^7F_4$ transitions, respectively.[50,54] The PL QYs of the samples with excitation at 250 nm are summarized in Table 1. The highest PL QY was obtained at the Eu concentration of 5 mol%. The PL QY increased with Eu concentration up to 5 mol% possibly because part of the excitation light at 250 nm was absorbed by the Cr^{3+} impurity ions. In fact, a nominally pure sample (without Eu dopant) had a PL QY of 35.9%. The lower PL QYs at Eu concentrations higher than 5 mol% are attributed to concentration quenching. The Eu concentration dependence of the PL QY in this study is similar to that of Eu-doped GAGG single crystals in a previous study, where the PL QY of 100% was achieved for Eu concentrations of 5 and 10 mol%.[50]

The XRL spectrum of Eu-doped GAGG nanoparticles with a Eu concentration of 5 mol% is shown in Fig. 4. Similar XRL spectra were observed for other Eu-doped nanoparticles. The spectrum had dominant peaks at 590 and 710 nm and a small peak at 810 nm with shoulders at 610, 630, 650, 690, and 730 nm. Except for the small peak at 820 nm and the shoulder at 740 nm, the peaks and shoulders are attributed to the same electronic transitions as those of the PL spectrum. The shoulder at 730 nm and the small peak at 820 nm are attributed to $^5D_0 \rightarrow {}^7F_5$ and $^5D_0 \rightarrow {}^7F_6$, respectively.[54] Judged from the XRL spectrum, we succeeded in the development of red-emitting scintillator nanoparticles.

From the viewpoint of estimating the scintillation light yield, the measurement of the pulse height spectra is effective. For this measurement, the long emission lifetime expected from the

Table 1
PL QY of samples.

Eu concentration (mol% to (Gd + Eu))	0.1	1	3	5	10	50	100
PL QY (%)	45.8	76.2	84.3	98.4	80.0	55.2	14.3

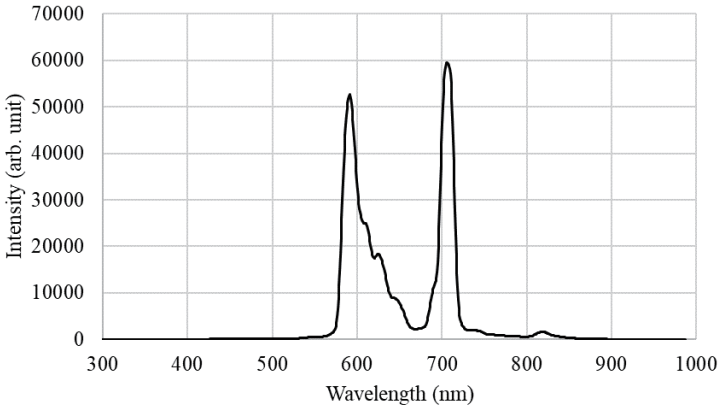

Fig. 4. XRL spectrum of Eu-doped GAGG nanoparticles with Eu concentration of 5 mol%.

4f–4f transition of Eu^{3+} ions in the nanoparticles is an issue, although a measurement system for the pulse height spectra of the scintillators having a slow scintillation decay has recently been developed to estimate the scintillation light yields of such scintillators.(56) Another issue is that the samples are in nanoparticle powder form. Owing to these issues, it is difficult to obtain a clear full-energy peak in the pulse height spectra of the samples. According to a previous report,(57) the scintillation light yield is proportional to the product of the energy transfer efficiency from the host to the luminescent centers and the QY of the PL of the luminescent centers. If we assume that the energy transfer efficiency does not change with Eu concentration at 3–10 mol%, 5 mol% is also optimum for the scintillation. This consideration is in line with the results of Eu-doped GAGG single crystals having the highest scintillation light yield at 5 mol% doping.(49) Because the light collection efficiencies may be different for the different samples because of the incomplete light collection during the measurements, the quantitative estimation of the scintillation light yield based on the XRL intensity was difficult. Taking into account this difficulty, the scintillation light yields of the Eu-doped GAGG nanoparticles are roughly estimated to be comparable to those of Ce-doped GAGG nanoparticles.

4. Conclusions

We have developed scintillator nanoparticles based on Eu-doped GAGG. The nanoparticles were synthesized by a sol–gel method using tartaric acid. The size of the nanoparticles was less than 300 nm. Emission in the red wavelength region was successfully obtained in the PL and XRL. The PL QY of as high as 98.4% was obtained with the Eu concentration of 5 mol%. On the basis of these results, we have succeeded in the development of red-emitting scintillator nanoparticles.

Acknowledgments

This research was supported by a Grant-in-Aid for Scientific Research (A) (22H00308, 2022–2025). Part of this research is based on the Cooperative Research Project of the Research Center for Biomedical Engineering, Ministry of Education, Culture, Sports, Science and Technology of Japan.

References

1 M. Koshimizu: Jpn. J. Appl. Phys. **62** (2023) 010503.
2 M. Koshimizu: J. Lumin. **278** (2025) 121008.
3 N. Hayashi and M. Koshimizu: J. Lumin. **277** (2025) 120993.
4 T. Yanagida: Proc. Jpn. Academy Ser. B **94** (2018) 75.
5 T. Yanagida, T. Kato, D. Nakauchi, and N. Kawaguchi: Jpn. J. Appl. Phys. **62** (2023) 010508.
6 N. Kawano, M. Koshimizu, G. Okada, Y. Fujimoto, N. Kawaguchi, T. Yanagida, and K. Asai: Sci. Rep. **7** (2017) 14754.
7 R. Nagaoka, N. Kawano, Y. Takebuchi, H. Fukushima, T. Kato, D. Nakauchi, and T. Yanagida: Jpn. J. Appl. Phys. **62** (2023) 110601.
8 T. Suto, N. Kawano, K Okazaki, Y Takebuchi, H. Fukushima, T. Kato, D. Nakauchi, and T. Yanagida: Jpn. J. Appl. Phys. **62** (2023) 010610.
9 T. Suto, N. Kawano, K. Okazaki, K. Ichiba, Y. Takebuchi, T. Kato, D. Nakauchi, and T. Yanagida: Jpn. J. Appl. Phys. **63** (2024) 01SP17.
10 M. Koshimizu: Funct. Mater. Lett. **13** (2020) 2030003.
11 F. Hiyama, T. Noguchi, M. Koshimizu, S. Kishimoto, R. Haruki, F. Nishikido, Y. Fujimoto, T. Aida, S. Takami, and T. Adschiri, K. Asai: Jpn. J. Appl. Phys. **57** (2018) 052203.
12 A. Sato, Y. Fujimoto, K. Asai, and M. Koshimizu: Jpn. J. Appl. Phys. **63** (2024) 01SP06.
13 H. Tsukahara, Y. Fujimoto, K. Asai, and M. Koshimizu: J. Lumin. **271** (2024) 120592.
14 H. Fukushima, D. Nakauchi, T. Kato, N. Kawaguchi, and T. Yanagida: Jpn. J. Appl. Phys. **62** (2023) 010506.
15 D. Nakauchi, T. Kato, N. Kawaguchi, and T. Yanagida: Jpn. J. Appl. Phys. **62** (2023) 010607.
16 Y. Shao, R. L. Conner, N. R. S. Souza, R. S. Silva, and L. G. Jacobsohn: Jpn. J. Appl. Phys. **62** (2023) 010601.
17 A. Ito, S. Matsumoto: Jpn. J. Appl. Phys. **62** (2023) 010612.
18 D. Yuan, F. G Víllora, N. Kawaguchi, D. Nakauchi, T. Kato, T. Yanagida, and K. Shimamura: Jpn. J. Appl. Phys. **62** (2023) 010614.
19 H. Fukushima, D. Nakauchi, T. Kato, N. Kawaguchi, and T. Yanagida: Sens. Mater. **35** (2023) 429.
20 D. Shiratori, H. Fukushima, D. Nakauchi, T. Kato, N. Kawaguchi, and T. Yanagida: Sens. Mater. **35** (2023) 439.
21 P. Kantuptim, T. Kato, D. Nakauchi, N. Kawaguchi, K. Watanabe, and T. Yanagida: Sens. Mater. **35** (2023) 451.
22 K. Okazaki, D. Nakauchi, H. Fukushima, T. Kato, N. Kawaguchi, and T. Yanagida: Sens. Mater. **35** (2023) 459.
23 D. Nakauchi, F. Nakamura, T. Kato, N. Kawaguchi, and T. Yanagida: Sens. Mater. **35** (2023) 467.
24 T. Kunikata, P. Kantuptim, D. Shiratori, T. Kato, D. Nakauchi, N. Kawaguchi, and T. Yanagida: Sens. Mater. **36** (2024) 457.
25 Y. Endo, K. Ichiba, D. Nakauchi, T. Kato, N. Kawaguchi, and T. Yanagida: Sens. Mater. **36** (2024) 473.
26 H. Kimura, H. Fukushima, K. Watanabe, T. Fujiwara, H. Kato, M. Tanaka, T. Kato, D. Nakauchi, N. Kawaguchi, and T. Yanagida: Sens. Mater. **36** (2024) 507.
27 K. Okazaki, D. Nakauchi, P. Kantuptim, T. Kato, N. Kawaguchi, and T. Yanagida: Jpn. J. Appl. Phys. **63** (2024) 01SP02.
28 Y. Takebuchi, D. Shiratori, T. Kato, D. Nakauchi, N. Kawaguchi, and T. Yanagida: Sens. Mater. **35** (2023) 507.
29 T. Kunikata, T. Kato, D. Shiratori, P. Kantuptim, D. Nakauchi, N. Kawaguchi, and T. Yanagida: Sens. Mater. **35** (2023) 491.
30 Y. Nakabayashi, Y. Fujimoto, M. Koshimizu, H. Kawamoto, and K. Asai: J. Mater. Sci.: Mater. Electron. **35** (2024) 575.
31 Y. Fujimoto and K. Asai: Jpn. J. Appl. Phys. **62** (2023) 010605.
32 N. Kawaguchi, T. Kato, D. Nakauchi, and T. Yanagida: Jpn. J. Appl. Phys. **62** (2023) 010611.
33 K. Miyazaki, D. Nakauchi, T. Kato, N. Kawaguchi, and T. Yanagida: Sens. Mater. **36** (2024) 515.
34 K. Yamabayashi, K. Okazaki, D. Nakauchi, T. Kato, N. Kawaguchi, and T. Yanagida: Sens. Mater. **36** (2024) 523.

35 T. Kato, D. Nakauchi, N. Kawaguchi, and T. Yanagida: Sens. Mater. **36** (2024) 531.
36 H. Kimura, T. Fujiwara, M. Tanaka, T. Kato, D. Nakauchi, N. Kawaguchi, and T. Yanagida: Sens. Mater. **35** (2023) 513.
37 K. Miyazaki, D. Nakauchi, T. Kato, N. Kawaguchi, and T. Yanagida: J. Mater. Sci.: Mater. Electron. **34** (2023) 1082.
38 M. Ishida, A. Watanabe, H. Kawamoto, Y. Fujimoto, and K. Asai: J. Mater. Sci.: Mater. Electron. **35** (2024) 1743.
39 S. Otake, T. Kato, D. Nakauchi, N. Kawaguchi, and T. Yanagida: J. Lumin. **275** (2024) 120828.
40 A, Kamkaew, F. Chen, Y. Zhan, and R. L. Majewski, W. Cai: ACS Nano **10** (2016) 3918.
41 Z. Hong, Z. Chen, Q. Chen, and H. Yang: Acc. Chem. Res. **56** (2023) 37.
42 T. Matsubara, T. Yanagida, N. Kawaguchi, T. Nakano, J. Yoshimoto, M. Sezaki, H. Takizawa, S. P. Tsunoda, S. Horigane, S. Ueda, S. Takemoto-Kimura, H. Kandori, A. Yamanaka, and T. Yamashita: Nat. Commun. **12** (2021) 4478.
43 M. Koshimizu, Y. Fujimoto, and K. Asai: Sens. Mater. **35** (2023) 521.
44 M. Hildebrandt, M. Koshimizu, Y. Asada, K. Fukumitsu, M. Ohkuma, N. Sang, T. Nakano, T. Kunikata, K. Okazaki, N. Kawaguchi, T. Yanagida, L. Lian, J. Zhang, and T. Yamashita: Int. J. Mol. Sci. **25** (2024) 11365.
45 P. Sengar, K. García-Tapia, B. Can-Uc, K. Juárez-Moreno, O. E. Contreras-López, and G. A. Hirata: J. Appl. Phys. **126** (2019) 083107.
46 A. C. S. Hamilton, G. I. Lampronti, S. E. Rowley, and S. E. Dutton: J. Phys.: Condens. Matter **26** (2014) 116001.
47 J. Åhman. G. Svensson, and J. Albertsson: Acta Crystallogr., Sect. C: Cryst. Struct. Commun. **52** (1996) 1336.
48 D. du Boulay, N. Ishizawa, and E. N. Maslen: Acta Crystallogr., Sect. C: Cryst. Struct. Commun.**60** (2004) i120.
49 T. Kunikata, K. Watanabe, P. Kantuptim, K. Ichiba, D. Shiratori, T. Kato, D. Nakauchi, N. Kawaguchi, and T. Yanagida: Jpn. J. Appl. Phys. **63** (2024) 01SP18.
50 R. D. Shannon: Acta Cryst. A **32** (1976) 751.
51 S. R. Rotman, C. Warde. H. L. Tuller, and J. Haggerty: J. Appl. Phys. **66** (1989) 3207.
52 C. R. Varney, S. M. Reda, D. T. Mackay, M. C. Rowe, and F. A. Selim: AIP Adv. **1** (2011) 042170.
53 J. Sua, Q. L. Zhangb, S. F. Shaob, W. P. Liub, S. M. Wanb, and S. T. Yin: J. Alloy Compd. **470** (2009) 306.
54 I. E. Kolesnikov, D. V. Tolstikova, A. V. Kurochkin, A. A. Manshina, and M. D. Mikhailov: Opt. Mater. **37** (2014) 306.
55 A. Ćirić, L. Marciniak, and M. D. Dramićanin: Sci. Rep. **12** (2022) 563.
56 K. Watanabe, T. Yanagida, D. Nakauchi, and N. Kawaguchi: Jpn. J. Appl. Phys. **60** (2021) 106002.
57 D. J. Robbins: J. Electrochem. Soc. **127** (1980) 2694.